Copolymer Photocatalysts for Visible-Light-Driven Hydrogen Evolution

Conjugated polymers with an all-acceptor design featuring enhanced electron output sites and compact network structures offer a solution to improve the efficiency of the photocatalytic hydrogen evolution reaction.

To effectively address the challenges of climate change, an urgent transition from fossil fuels to carbon-neutral energy sources is essential. Despite the abundance of solar energy as a renewable resource, its intermittent nature poses obstacles in meeting on-demand energy needs. An optimal solution involves storing solar energy through chemical fuel bonds, with photocatalytic hydrogen evolution gaining prominence as a method to convert solar energy into hydrogen. In the past five years, conjugated polymers have emerged as promising candidates due to their structural diversity, modular functionality, environmental friendliness, and tuneable energy levels (**Fig. 1(a)**). However, a critical drawback exists in the insufficient tentacles for electron output in these polymers. These tentacles play a crucial role in efficiently directing and concentrating electrons for interactions with cocatalysts or protons, thereby influencing photocatalytic performance. Previous efforts have concentrated on donor–acceptor (D–A) type conjugated polymers, integrating electron-output functional groups on the acceptor unit. However, this approach restricts the number of electron-output functional groups, resulting in over 50% of the conjugated polymer unit lacking these essential tentacles.

U-Ser Jeng (NSRRC) and Ho-Hsiu Chou (National Tsing Hua University) introduced four novel oxidized ladder-type heteroarenes that incorporate dibenzo[b,d] thiophene 5,5-dioxide to fabricate all-acceptor (A_1–A_2)-type conjugated polymers, specifically named PBDTTFSOS, PBDTTTSOS, PIDDSOS, and PITDSOS.[1] These A_1–A_2-type conjugated polymers facilitate the direct combination of two conjugated monomers with electron-output sites, resulting in conjugated polymers featuring a higher density of electron-output sites compared to conventional D–A-type conjugated polymers. The increased electron-output site density is attributed to the presence of electron-output sites in both conjugated monomers. As part of the experimental controls, four D–A-type conjugated polymers with similar structures were also synthesized, designated as PBDTTFS, PBDTTTS, PIDS, and PITS (**Fig. 1(b)**). As shown in **Figs. 2(a) and 2(b)** in next page, A_1–A_2-type conjugated polymers have demonstrated significant efficiency improvements, ranging from two to three orders of magnitude, when compared to their D–A-type conjugated polymer counterparts. To understand why the photocatalytic activity of A_1–A_2-type conjugated polymers is superior to that of D–A-type conjugated polymers, a combination of small-angle X-ray scattering (SAXS) and ultrasmall-angle X-ray scattering (USAXS) measurements were conducted at **TPS 13A**. In the low-q region of USAXS spanning from 0.002 to 0.006 $Å^{-1}$, defined by the scattering vector q based on X-ray wavelength (λ) and scattering angle (2θ), A_1–A_2-type conjugated polymers—namely PBDTTFSOS, PBDTTTSOS, PIDDSOS, and PITDSOS—demonstrated consistent power-law scattering behavior, expressed as I(q) ∝ q^α. The corresponding fitted α values were −3.54, −3.14, −3.76, and −3.38, respectively. By contrast, D–A-type conjugated polymers—PBDTTFS, PBDTTTS, PIDS, and PITS—exhibited relatively smaller α values of −2.96, −2.83, −3.51, and −3.23, respectively (**Figs. 2(c) and 2(d)**). These results indicate that A_1–A_2-type conjugated polymers form more compact network

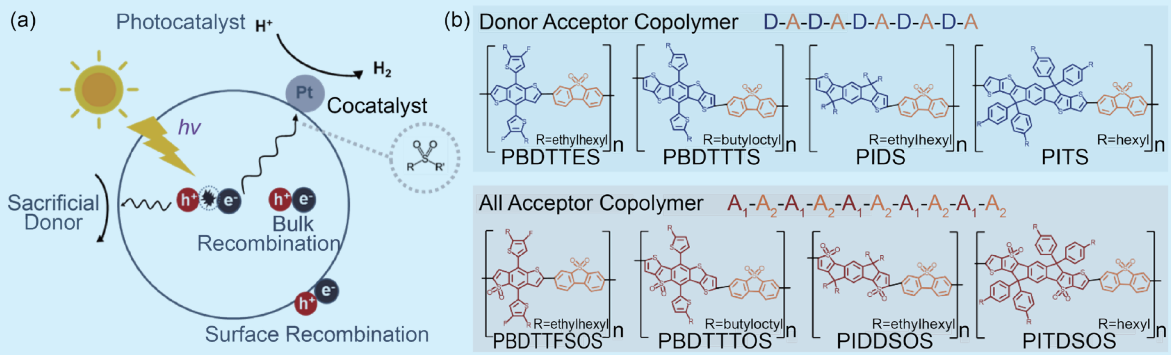

Fig. 1: (a) Schematic diagram of polymeric photocatalyst for photocatalytic hydrogen evolution from water, and (b) chemical compositions and molecular structures of the fabricated polymeric photocatalysts. [Reproduced from Ref. 1]

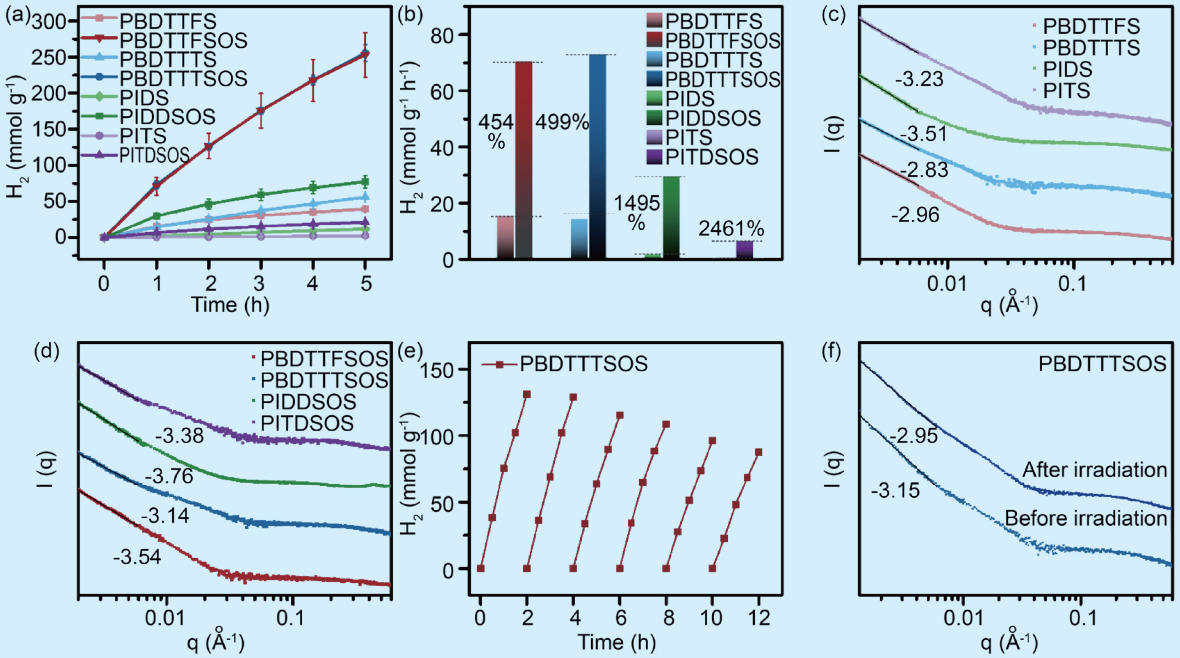

Fig. 2: (a) Time-dependent HER of the photocatalysts under visible-light illumination, (b) comparison of the HER between D–A-type conjugated polymers and A_1–A_2-type conjugated polymers, (c) combined USAXS (0.002–0.006 Å^{-1}) and SAXS data of the D–A-type conjugated polymers, (d) parallel USAXS–SAXS data of the corresponding A_1–A_2-type conjugated polymers, (e) photocatalytic cycling stability test of PBDTTTSOS; and (f) combined USAXS (0.002–0.006 Å^{-1}) and SAXS data of PBDTTTSOS before and after photocatalytic reaction. [Reproduced from Ref. 1]

structures in the solution of the hydrogen evolution reaction. Recent research suggests that the kinetics of hydrogen formation favor interactions between hydrogen atoms on different polymer chains rather than within the same polymer chain. Consequently, the observed superior efficiency in the hydrogen evolution reaction for A_1–A_2-type conjugated polymers compared to D–A-type conjugated polymers can be attributed to the more compact network structure formed in the reaction solution. To evaluate the stability of PBDTTTSOS in a photocatalytic hydrogen evolution reaction, the team conducted a continuous six-cycle experiment involving visible-light irradiation in an NMP/water/ascorbic acid (AA) mixture. The results indicated a gradual decrease in the quantity of generated hydrogen over the six cycles, with approximately 70% of the initial hydrogen evolution rate (HER) sustained after the sixth cycle. PBDTTTSOS maintained an HER of 48.6 mmol h^{-1} g^{-1} (**Fig. 2(e)**). To gain deeper insights into the efficiency decline, the team utilized USAXS and SAXS techniques to examine morphological and compactness changes post-photocatalytic reaction. Further analysis revealed that PBDTTTSOS underwent morphological alterations in the NMP/water/AA mixed solution, leading to a more loosely packed network following the hydrogen evolution reaction. Specifically, the USAXS analysis indicated a reduction in the α value from –3.14 (as prepared) to –2.88 post-photocatalytic activity (**Fig. 2(f)**). Moreover, the self-inhibition phenomenon of AA and its oxidation product dehydroascorbic acid (DHA) emerged as a contributing factor to the overall decrease in hydrogen evolution efficiency. In summary, these findings suggest that the observed reduction in photocatalytic efficiency can be attributed to morphological changes in PBDTTTSOS within the NMP/water/AA mixture, along with the self-inhibition effects of AA and its oxidation product DHA.

To date, the majority of reported polymer photocatalysts have relied on freshwater as the primary source for hydrogen evolution, posing a significant challenge due to the limited availability of freshwater resources (< 1% of Earth's water). This scarcity exacerbates an already critical global challenge. Therefore, a promising avenue involves the direct splitting of seawater without purification, capitalizing on its abundance (> 96.5% of Earth's water) for sustainable solar-to-hydrogen energy conversion. PBDTTFSOS and PBDTTTSOS were chosen as representative compounds for investigating photocatalytic hydrogen evolution through seawater splitting under visible-light irradiation. In simulated seawater, PBDTTFSOS and PBDTTTSOS exhibited an impressive HER rate of 86.9 and 92.6 mmol g^{-1} h^{-1}, marking a 23.0% and 27.0% increase compared to that observed in deionized (DI) water (**Figs. 3(a) and 3(b)**). The concurrent USAXS–SAXS analysis revealed more compact network structures of the polymers in the aqueous solution with 0.6 M NaCl. Specifically, the USAXS data for PBDTTTSOS in simulated seawater exhibited a larger α value of –3.42, in contrast to –3.14 in DI water. This indicates a more compact chain packing density of polymer chains in simulated seawater, elucidating the enhanced photocatalytic efficiency observed in this medium (**Fig.**

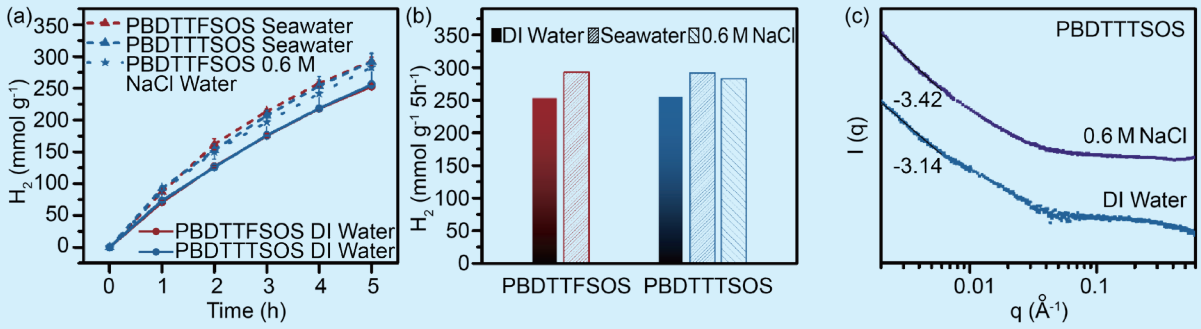

Fig. 3: (a) Temporal evolution of the HER for PBDTTFSOS and PBDTTTSOS under visible-light exposure in DI water, simulated seawater (0.6 M NaCl solution), and natural seawater solution, (b) comparative analysis of the HER for PBDTTFSOS and PBDTTTSOS in DI water, simulated seawater (0.6 M NaCl solution), and natural seawater solution, and (c) combined USAXS and SAXS of PBDTTTSOS in DI water and simulated seawater solutions. DI water solution conditions: 2 mg photocatalyst, 1 M AA, 9 mL DI water, 1 mL NMP, pH 4, 3 wt% H_2PtCl_6. Simulated seawater solution conditions: 2 mg photocatalyst, 1 M AA, 9 mL DI water, 0.6 M NaCl, 1 mL NMP, pH 4, 3 wt% H_2PtCl_6. Natural seawater solution conditions: 2 mg photocatalyst, 1 M AA, 9 mL natural seawater, 1 mL NMP, pH 4, 3 wt% H_2PtCl_6. [Reproduced from Ref. 1]

3(c)).

In summary, the synthesis of four A_1–A_2-type conjugated polymers has demonstrated a remarkable improvement in efficiency ranging from 454% to 2461% when compared to their conventional D–A-type conjugated polymer counterparts. Advanced morphological analyses have unveiled the superior capability of A_1–A_2-type conjugated polymers in establishing compact network structures during photocatalytic hydrogen evolution reactions. These findings underscore the potential of A_1–A_2-type conjugated polymers as highly effective and promising materials for enhancing the efficiency of hydrogen evolution processes. (Reported by Wei-Cheng Lin and Ho-Hsiu Chou, National Tsing Hua University)

This report features the work of Ho-Hsiu Chou and his collaborators published in Small ***19****, 2302682 (2023).*

TPS 13A Biological Small-angle X-ray Scattering

- Small- and Ultrasmall-angle X-ray Scattering
- Materials Science, Polymer

Reference

1. W. C. Lin, C. L. Chang, C. H. Shih, W. C. Lin, Z. Y. Lai, J. W. Chang, L.Y. Ting, T. F. Huang, Y. E. Sun, H. Y. Huang, Y. T. Lin, J. J. Liu, Y. H. Wu, Y. T. Tseng, Y. R. Zhuang, B. H. Li, A. C. Su, C. H. Yu, C. W. Chen, K. H. Lin, U. S. Jeng, H. H. Chou, Small **19**, 2302682 (2023).